

# Probing the I<sub>c</sub>e–N<sub>c</sub>–I phase transitions in a lyotropic liquid crystal by the surface plasmon resonance of embedded gold nanoparticles

V.M. Lenart, R.F. Turchiello & S.L. Gómez

**To cite this article:** V.M. Lenart, R.F. Turchiello & S.L. Gómez (2016): Probing the I<sub>c</sub>e–N<sub>c</sub>–I phase transitions in a lyotropic liquid crystal by the surface plasmon resonance of embedded gold nanoparticles, *Liquid Crystals*, DOI: [10.1080/02678292.2016.1162859](https://doi.org/10.1080/02678292.2016.1162859)

**To link to this article:** <http://dx.doi.org/10.1080/02678292.2016.1162859>



Published online: 30 Mar 2016.



Submit your article to this journal 



Article views: 7



View related articles 



View Crossmark data 

Full Terms & Conditions of access and use can be found at  
<http://www.tandfonline.com/action/journalInformation?journalCode=tlct20>

# Probing the I<sub>RE</sub>–N<sub>C</sub>–I phase transitions in a lyotropic liquid crystal by the surface plasmon resonance of embedded gold nanoparticles

V.M. Lenart<sup>a</sup>, R.F. Turchiello<sup>b</sup> and S.L. Gómez<sup>a</sup>

<sup>a</sup>Department of Physics, State University of Ponta Grossa, Ponta Grossa, Brazil; <sup>b</sup>Department of Physics, Federal University of Technology of Paraná, Ponta Grossa, Brazil

## ABSTRACT

The surface plasmon resonance of noble metal nanoparticles depends on properties of the nanoparticles and of the surrounding medium, which make it a suitable probe of the local ordering of anisotropic media. Besides that, no much attention was paid to the possibility of using the surface plasmon resonance as probe of phase transitions in liquid crystals. In this work, we have used the surface plasmon resonance of rather spherical Au nanoparticles of  $(12 \pm 2)$  nm for studying the phase transitions of a lyotropic liquid crystal of potassium laurate, 1-decanol and water that exhibits the phase sequence I<sub>RE</sub>–N<sub>C</sub>–I on rising temperature. The wavelength of the surface plasmon resonance is blue-shifted sharply at the I<sub>RE</sub> → N<sub>C</sub> transition, remaining almost constant at the N<sub>C</sub> → I transition. The behaviour at the low-temperature transition can be assigned to a change in the shape anisotropy of the micelles. On the contrary, at the higher temperature transition, the local environment of the nanoparticles remains unmodified.

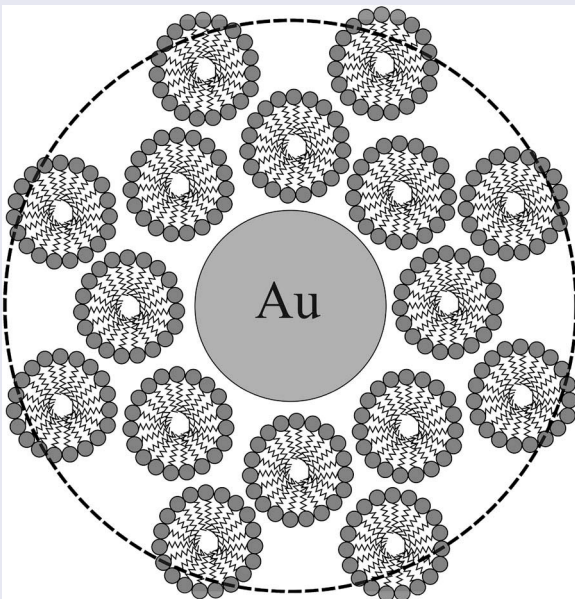
## ARTICLE HISTORY

Received 12 January 2016

Accepted 3 March 2016

## KEYWORDS

plasmonic nanoparticle;  
lyotropic liquid crystal;  
phase transition



## 1. Introduction

The linear and nonlinear optical properties of colloidal noble metals attracted enormous interest in recent years due to the new phenomena rising from the nanoscale dimensions and technological possibilities. These properties arise mainly from the localised surface plasmon (SP), a non-propagating collective excitation of conduction band electrons coupled to an electromagnetic field that is excited by direct light

illumination.[1] The resonance of the surface plasmon (SPR) is highly dependent on the dielectric constant of the surrounding medium [2] being sensible to changes within 20 nm from the nanoparticle surface.[3] Due to that penetration depth of the evanescent field of the localised surface plasmon, the SPR can probe the changes in the microenvironment of the particle. The SPR of noble metal nanoparticles has been employed as a probe for changes in ordering of anisotropic media.

Previous works showed that different anchoring conditions of thermotropic liquid crystals on a thin film of gold [4] or on gold nanorods [5] lead to changes in the SPR. The N-I transitions of a thermotropic liquid crystals have also been detected previously by the surface plasmon technique.[6] Also, it has been shown that SPR of gold nanoparticles (AuNPs) immobilised on a surface couples strongly to the local order in thermotropic liquid crystals.[7,8] Conversely, AuNPs allowed to control optically the reorientation of thermotropic liquid crystals via a plasmon-enhanced local field effect,[9] and a non-radiative relaxation of the SPR has been employed in the treatment of tumours. [10,11] Despite being suitable to probe microenvironments, the SPR of noble metal nanoparticles has not been employed yet for studying the rich polymorphism of lyotropic mesophases, systems formed by a mixture of amphiphilic molecules and a solvent. The basic units of these systems are molecular aggregates spontaneously formed by the interplay of hydrophobic and hydrophilic interactions, whose shapes are controlled by physico-chemical parameters like relative concentrations and temperature.[12] In this article we present, to our knowledge, the first experimental study showing the use of the SPR of metallic nanoparticles to determine the phase transition temperature of a lyotropic liquid crystal (LLC). The article is organised as follows: Section 2 presents the fundamentals of plasmonics. Section 3 describes the experimental details about preparation and characterisation of the samples. Section 4 presents the experimental results and discussions. Finally, Section 5 summarises our findings.

## 2. Fundamentals

The optical properties of metals, over a wide range of frequencies, can be properly described by the free electron gas model. In this model, a gas of free electrons of number density  $n$  moves against the background of fixed positive ion cores. The forced oscillations of the electrons due to the electromagnetic field are damped via collisions with characteristic frequency  $\gamma = \tau^{-1}$ , where  $\tau$  is the characteristic relaxation time, which for gold is  $\sim 10^{-14}\text{s}$ .[13] In the Drude model, the real and imaginary components of the complex dielectric constant of a metal,  $\epsilon(\omega) = \epsilon_1(\omega) + i\epsilon_2(\omega)$ , are given by

$$\epsilon_1(\omega) = 1 - \frac{\omega_p^2}{\omega^2 + \gamma^2}, \quad (1)$$

$$\epsilon_2(\omega) = \frac{\omega_p^2 \gamma}{\omega^3 + \omega \gamma^2}, \quad (2)$$

where  $\omega_p = \frac{n e^2}{\epsilon_0 m}$  is the plasma frequency of the free electron gas ( $\sim 10^{16}\text{rad/s}$ ). In the visible range of spectrum,  $\omega \gg \gamma$  and the dielectric constant is almost real, given approximately by

$$\epsilon(\omega) = 1 - \frac{\omega_p^2}{\omega^2}, \quad (3)$$

However, interband transitions occurring in the visible range in noble metals limit this approach. Following Maier's formalism,[14] the optical properties (absorption and scattering cross-sections) of metallic nanoparticles of size  $d$  can be obtained within the framework of electromagnetism under the quasi-static approximation provided  $d \ll \lambda$ .[15] In this way, the nanoparticle can be considered immersed in a homogeneous electric field. The absorption cross-section  $\sigma_{abs}$  of spherical particles of radius  $a$  immersed in a medium of dielectric constant  $\epsilon_m$  under illumination with light of wave number  $k$  is given by

$$\sigma_{abs} = 4\pi k a^3 \text{Im} \left[ \frac{\epsilon - \epsilon_m}{\epsilon + 2\epsilon_m} \right]. \quad (4)$$

A resonant condition is obtained by minimising the modulus of the denominator. For a slowly varying condition of  $\epsilon$  around the resonance frequency, the minimum is arrived at if

$$\epsilon = -2\epsilon_m, \quad (5)$$

known as Fröhlich condition.

## 3. Experimental details

The lyotropic liquid crystal used in this work was a ternary mixture with the following composition: potassium laurate (29.40 wt%), 1-decanol (6.60 wt%) and water (64.00 wt%). The phase sequence determined by polarised light microscopy on heating was: Reentrant Isotropic (I<sub>RE</sub>)–Calamitic Nematic (N<sub>C</sub>)–Isotropic (I). The nanoparticles of gold were prepared by the standard Turkevich's method.[16] There were used 20 ml of 1.0 mM of HAuCl<sub>4</sub> · H<sub>2</sub>O (Vetec PA) as precursor and 2.0 ml of a 1% solution of Na<sub>3</sub>C<sub>6</sub>H<sub>5</sub>O<sub>7</sub> · 2H<sub>2</sub>O (Synth PA) as reductor and surfactant agent, respectively. These reagents were used without further purification. The temperature during the reaction was maintained close to 100°C. Measurement of zeta potential reveals an average surface charge of  $-33.4 \pm 0.5\text{ mV}$  at pH = 8.2. The colloid remained stable, protected from the light, for at least 5 months. The concentration of AuNPs in the lyotropic liquid crystals was about  $8.5 \times 10^{11}$  nanoparticles/ml. The transition temperature of the AuNP-doped lyotropic liquid crystal

was determined by processing the images obtained by polarised light microscopy. This technique registers the light produced by an unpolarised source and transmitted by the sample positioned between 90°C-crossed linear polarisers (polarizer and analyser). For that purpose, the sample was conditioned in a 200-μm-thick microslide and the rather homogeneous alignment of the N<sub>C</sub> phase with the average alignment direction (optical axis) along the length of the microslide was induced spontaneously by flux. Temperature was controlled with precision of 0.01°C (Hot Stage mk1000, Instec). The UV-Vis spectrum of the sample as a function of temperature was obtained with a spectrophotometer with control of temperature facilities (Cary 50, Varian) and which uses an unpolarised light source and a quartz cuvette with 10 mm pathlength. For these measurements we exercised the following cautions: (i) for avoiding water condensation on the walls of the quartz cell at low temperatures, we used silica gel around the Peltier chamber; (ii) the equilibrium temperature was determined by two sensors at different positions inside the Peltier chamber when the difference were less than 0.2°C; (iii) the spectrum was acquired 7 min after the set temperature was reached.

#### 4. Results and discussions

Figure 1a shows a transmission electron microscopy (TEM) image of rather spherical nanoparticles with an average radius of  $12 \pm 2$  nm. Figure 1b displays a high-resolution TEM image (HRTEM) of one of the particles and the inset shows its fast Fourier transform (FFT) pattern, which corresponds to the known fcc arrangement of the gold.[17]

The N<sub>C</sub> phase of the liquid crystal is characterised by a long-range orientational order of the basic units, micelles in lyotropics and molecules in thermotropics, and optically it is birefringent. On the other hand, the isotropic phases (I<sub>RE</sub> and I) do not exhibit long-range orientational order. Textures obtained by polarised light microscopy of the phase sequence on heating are shown in Figure 2 along with the normalised transmittance as a function of temperature, defined as the average intensity of the pixels in each picture obtained with the scikit-image package of Python programming language.[18,19] It is possible to see in Figure 2 a coexistence region at the two phase transitions, being possible to assign the following temperature ranges to the transitions:  $(14.5 \pm 2.5)^\circ\text{C}$  and  $(56.5 \pm 2.5)^\circ\text{C}$ , respectively. For mixtures of more than one kind of amphiphilic molecules, micelles in the N<sub>C</sub> phase are essentially bilayers with a prolate

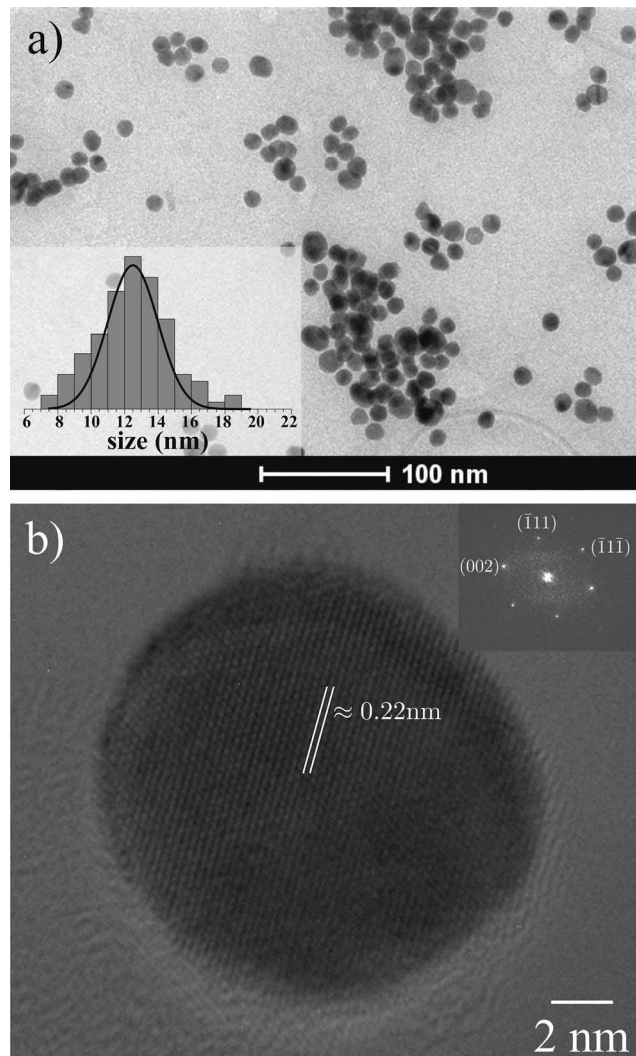


**Figure 1.** (a) TEM image of AuNPs obtained by Turkevich's method with average radius of 12 nm; (b) HRTEM of one particle. The inset shows its corresponding FFT pattern associated with the fcc arrangement and the interplanar spacing is about 0.22 nm, which is characteristic of gold.

symmetry (typical dimensions of  $\sim 100 \text{ \AA}$ ), suffering slight changes with temperature.[20] Further, in the isotropic regions of the phase diagram (I<sub>RE</sub> and I) that are in the neighbourhood of the nematic domain, micelles keep some characteristics observed in the nematic phase: (i) the intrinsically biaxial shape, and (ii) the local pseudolamellar ordering, with a correlation volume of about three micelles.

Figure 3 displays the UV-Vis spectrum of AuNPs dispersed in water at temperatures ranging from 16°C to 90°C. Upon raising of the temperature, the amplitude of the plasmon decreases but the wavelength at the maximum extinction ( $\sim 525 \text{ nm}$ ) does not change. On the other hand, the UV-Vis spectrum of the AuNPs immersed in the LLC for some representative temperatures are shown in Figure 4.

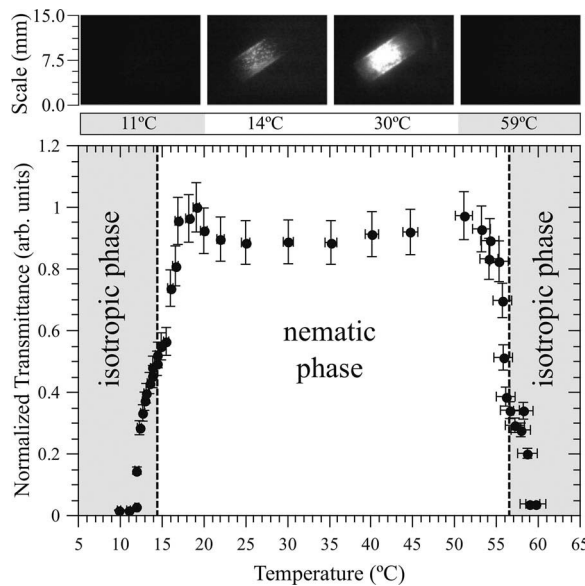


**Figure 2.** (Above) Some textures by polarised light microscopy of the AuNP-doped lyotropic liquid crystal at the  $I_{RE}$ ,  $N_C$  and  $I$  phases. Polariser and analyser are about  $0^\circ\text{C}$  and  $90^\circ\text{C}$  and the longitudinal axis is about  $45^\circ\text{C}$ . (Below) Normalised transmittance of the sample as a function of temperature.

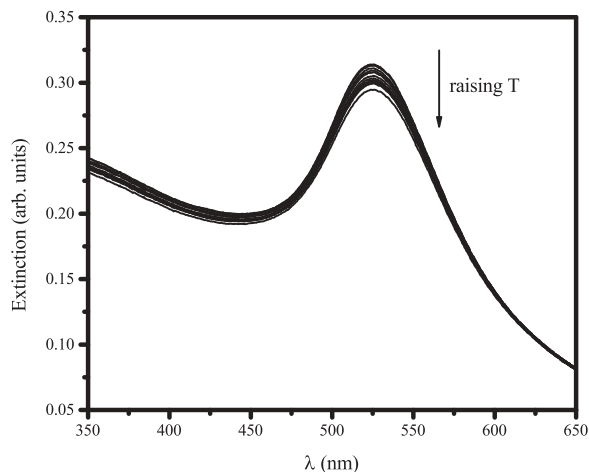


**Figure 3.** UV-Vis spectra of AuNPs in water at temperatures ranging from  $16^\circ\text{C}$  to  $90^\circ\text{C}$ .

The SPR of the AuNPs when immersed in the LLC in the nematic phase is red-shifted  $\sim 12$  nm and red-shifted  $\sim 24$  nm ( $I_{RE}$  phase) when compared to the SPR of AuNPs in water. At the frequency range of visible light, the modulus of the dielectric constant of gold increases by decreasing the frequency of the incident field.[13] The refractive indexes of the LLC are usually higher than that of water. On the other hand, we rule out a clustering process of the AuNPs as the origin of the small red-shift. It has been shown, both experimentally [21–23] and theoretically,[24] that aggregation

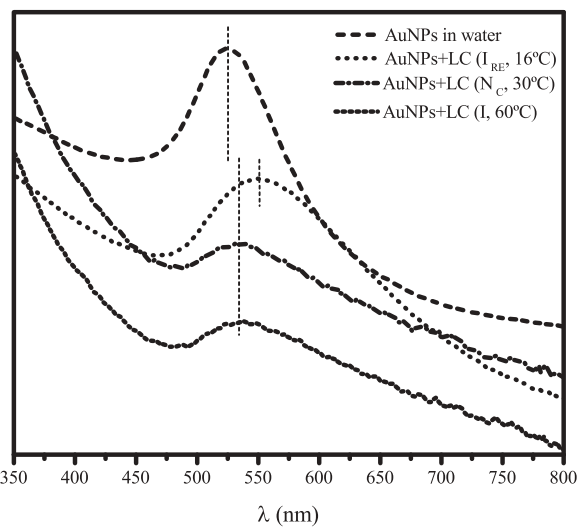


**Figure 4.** UV-Vis spectra of AuNPs in lyotropic liquid crystal at different temperatures ( $16^\circ\text{C}$ ,  $30^\circ\text{C}$  and  $60^\circ\text{C}$ ) and in water. Dotted vertical lines show the position of maximum extinction. Spectra are displaced vertically for better viewing.

usually shifts the spectrum to the red, leading to broader absorption bands centred at the range  $600\text{--}800$  nm. So, the higher wavelength at the maximum of the SPR in the LLC at any temperature could be assigned to the higher dielectric constant of the LLC but not to clustering of the AuNPs. It is worth mentioning that the analysis of the amplitude of the SPR is made difficult due to the intense scattering observed in the nematic phase. The wavelength at the maximum absorbance of the SPR ( $\lambda_{\max}$ ) as a function of temperature for the AuNPs embedded in the LLC is shown in Figure 5. As can be seen,  $\lambda_{\max}$  is blue-shifted  $\sim 12$  nm at the  $I_{RE}\text{-}N_C$  transition, going from  $\sim 549$  nm in the  $I_{RE}$  phase to  $\sim 537$  nm in both, the  $N_C$  phase.

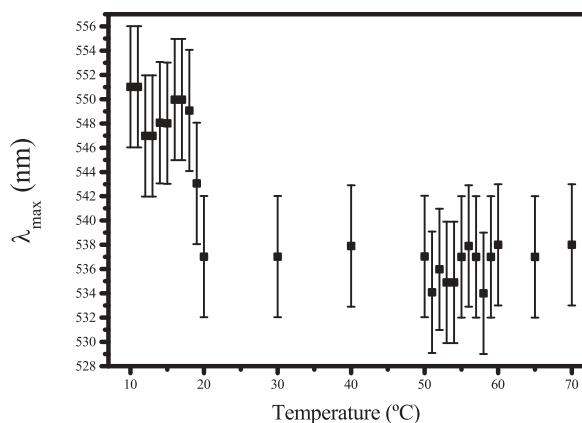


**Figure 5.** Wavelength at the maximum of the SPR of AuNPs embedded in the lyotropic liquid crystal as a function of temperature.

Furthermore, to the transition temperature can be assigned the value  $19 \pm 1^\circ\text{C}$ .

On the contrary, at the higher temperature transition ( $\text{N}_\text{C}-\text{I}$ ) is not observed any change in  $\lambda_{\max}$ . Usually, the less symmetric phase ( $\text{N}_\text{C}$  in our case) is found at a lower temperature than the isotropic phase, where thermal fluctuations lead to the loss of the long-range orientational order of the correlation volumes. Although symmetry requirements dictate that the nematic-isotropic transition must be of first order,[25] there are some experimental evidences of the tricritical character.[26,27] On the contrary, experimental results show that the lower temperature transition has a different critical universality class to that of the higher temperature transition.[28] The peculiarity of the lower temperature transition can be understood as follows. Lowering temperature from the  $\text{N}_\text{C}$  phase and going through the  $\text{N}_\text{C} \rightarrow \text{I}_{\text{RE}}$  transition, the probability of *cis* configurations of the paraffinic chains decreases increasing the thickness of the bilayer.[29] As a consequence, the shape anisotropy of the micelles is reduced, i.e. micelles become rounded. So, the behaviour of the SPR at this transition can be ascribed mainly to a change of the average dielectric constant of the surrounding medium around the nanoparticle due to a change in the shape anisotropy of the micelles. Taking into account the known dielectric constant of gold,[13] the blue shift of the SPR when the lyotropic liquid crystal goes from the  $\text{I}_{\text{RE}}$  to  $\text{N}_\text{C}$  phase corresponds to a diminution of the average dielectric constant of the medium. This result correlates with the observed reduction of the refractive index on heating from  $\text{I}_{\text{RE}}$  to  $\text{N}_\text{C}$ .[30] As mentioned previously, at the region of the  $\text{I}$  phase that is close to the  $\text{N}_\text{C}$  domain, micelles maintain the biaxial symmetry and the local pseudo-lamellar ordering, along with the correlation volume of about three micelles. So, there is no change of the microenvironment around the AuNPs.

A sketch of the neighbouring region of the gold nanoparticle probed by the SP is shown in Figure 6. The penetration depth of the SP coincides with the dimension of the correlation volume of the micelles. So, at the  $\text{N}_\text{C}-\text{I}$  transition, a change of the average dielectric constant probed by the AuNPs is not expected. On the other hand, optical measurements in oriented samples probe a macroscopic region, differently from the SPR. This is evident from comparing the transition regions in Figures 2 and 5. Value of  $\lambda_{\max}$  changes more sharply than optical transmittance, which makes it possible to determine the phase transition temperature with a better precision.

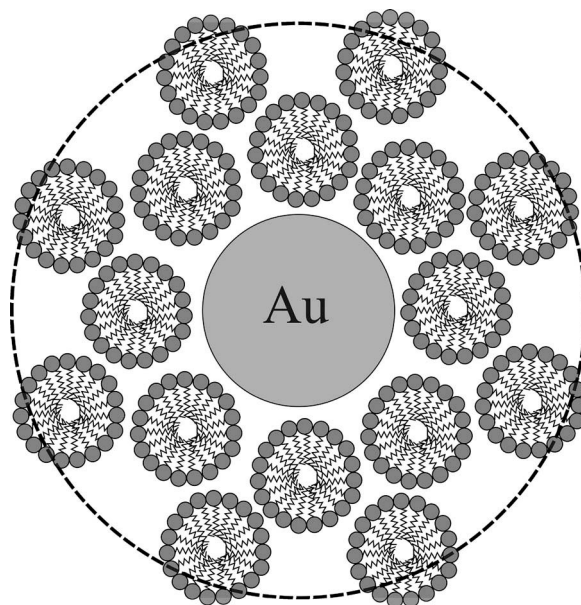


**Figure 6.** Sketch of the microenvironment of the gold nanoparticle probed by the SPR. The evanescent electromagnetic field of the SPR penetrates 20 nm inside the dielectric medium and micelles have a typical linear dimension of  $\sim 10$  nm.

## 5. Conclusions

In summary, we have shown that the SPR of AuNPs embedded in a lyotropic liquid crystal are suitable probes of phase transitions that involves changes in the shape of the micelles. In a ternary mixture of potassium laurate, 1-decanol and water, which exhibits the phase sequence  $\text{I}_{\text{RE}}-\text{N}_\text{C}-\text{I}$ , the wavelength of the SPR suffers a blue shift of about 12 nm at  $\text{I}_{\text{RE}} \rightarrow \text{N}_\text{C}$  transition. Additionally, at the  $\text{N}_\text{C} \rightarrow \text{I}$  transition, the wavelength of the SPR remains almost constant. This behaviour of the SPR is consistent with a change in the symmetry of the micelles at the lower temperature transition and with the maintenance of the pseudo-lamellar local order in the high-temperature transition. So, the SPR can be used as a tool for tracking changes in the anisotropy of micelles and to study phase transitions in lyotropic liquid crystal without the necessity of a macroscopically ordered sample. In addition, this technique reduces the uncertainty in the determination of the phase transition temperature compared to the polarised light microscopy technique.

## Disclosure statement

No potential conflict of interest was reported by the authors.

## Funding

This work had the financial support of the Brazilian agencies CAPES, CNPq, Fundação Araucária and the Secretaria de

Ciência, Tecnologia e Ensino Superior do Governo do Paraná, and of the National Institute of Science and Technology in Complex Fluids (INCT-FCx). V. M. Lenart also acknowledges fellowship from CAPES [Proc. n°2263-13-0].

## References

- [1] Quinten M. Optical properties of nanoparticles systems: Mie and beyond. Singapore, Hong Kong: Wiley-VCH; 2011.
- [2] Link S, Mohamed MB, El-Sayed MA. Simulation of the optical absorption spectra of gold nanorods as a function of their aspect ratio and the effect of the medium dielectric constant. *J Phys Chem B*. 1999;103:3073–3077. doi:[10.1021/jp990183f](https://doi.org/10.1021/jp990183f).
- [3] Haes AJ, Zou S, Schatz GC, et al. A nanoscale optical biosensor: the long range distance dependence of the localized surface plasmon resonance of noble metal nanoparticles. *J Phys Chem B*. 2004;108:109–116. doi:[10.1021/jp0361327](https://doi.org/10.1021/jp0361327).
- [4] Evans SD, Allinson H, Boden N, et al. Surface plasmon resonance imaging of liquid crystal anchoring on patterned self-assembled monolayers. *J Phys Chem B*. 1997;101:2143–2148. doi:[10.1021/jp9633411](https://doi.org/10.1021/jp9633411).
- [5] Peroukidisa SD, Yannopapasb V, Vanakarasa AG, et al. Plasmonic response of ordered arrays of gold nanorods immersed within a nematic liquid crystal. *Liq Cryst*. 2014;41:1430–1435. doi:[10.1080/02678292.2014.923538](https://doi.org/10.1080/02678292.2014.923538).
- [6] Chu KC, Chen CK, Shen YR. Measurement of refractive-indexes and study of isotropicnematic phase transition by the surface-plasmon technique. *Mol Cryst Liq Cryst*. 1980;59:97–108. doi:[10.1080/00268948008073501](https://doi.org/10.1080/00268948008073501).
- [7] Koenig Jr GM, Gettelfinger BT, de Pablo JJ, et al. Using localized surface plasmon resonances to probe the nanoscopic origins of adsorbate-driven ordering transitions of liquid crystals in contact with chemically functionalized gold nanodots. *Nano Lett*. 2008;8:2362–2368. doi:[10.1021/nl801180c](https://doi.org/10.1021/nl801180c).
- [8] Koenig GM Jr, Meli MV, Park JS, et al. Coupling of the plasmon resonances of chemically functionalized gold nanoparticles to local order in thermotropic liquid crystals. *Chem Mater*. 2007;19:1053–1061. doi:[10.1021/cm062438p](https://doi.org/10.1021/cm062438p).
- [9] Shan J, Shi W, Liu LY, et al. Optical control of surface anchoring and reorientation of liquid crystals via a plasmon-enhanced local field. *Phys Rev Lett*. 2012;109:147801. doi:[10.1103/PhysRevLett.109.147801](https://doi.org/10.1103/PhysRevLett.109.147801).
- [10] Khlebtsov BN, Panfilova EV, Terentyuk GS, et al. Plasmonic nanopowders for photothermal therapy of tumors. *Langmuir*. 2012;28:8994–9002. doi:[10.1021/la300022k](https://doi.org/10.1021/la300022k).
- [11] Li JL, Gu M. Gold-nanoparticle-enhanced cancer photothermal therapy. *IEEE J Sel Top Quant*. 2010;16:989–996. doi:[10.1109/JSTQE.2009.2030340](https://doi.org/10.1109/JSTQE.2009.2030340).
- [12] Figueiredo Neto AM, Salinas SRA. The physics of lyotropic liquid crystals: phase transitions and structural properties. Oxford: Oxford University Press; 2005.
- [13] Johnson PB, Christy RW. Optical constants of noble metals. *Phys Rev B*. 1972;6:4370–4379. doi:[10.1103/PhysRevB.6.4370](https://doi.org/10.1103/PhysRevB.6.4370).
- [14] Maier SA. *Plasmonics: fundamentals and applications*. New York (NY): Springer; 2007.
- [15] Jackson JD. *Classical electrodynamics*. 3rd ed. New York (NY): John Wiley; 1999.
- [16] Turkevich J, Stevenson PC, Hillier J. A study of the nucleation and growth processes in the synthesis of colloidal gold. *Discuss Faraday Soc*. 1951;11:55. doi:[10.1039/df9511100055](https://doi.org/10.1039/df9511100055).
- [17] Chen Y, Gu X, Nie CG, et al. Shape controlled growth of gold nanoparticles by a solution synthesis. *Chem Comm*. 2005;33:4181–4183. doi:[10.1039/b504911c](https://doi.org/10.1039/b504911c).
- [18] van Rossum G. Python tutorial, technical report CS-R9526. Amsterdam: Centrum voor wiskunde en informatica (CWI); 1995.
- [19] van der Walt S, Schönberger JL, Nuñez-Iglesias J, et al., et al. scikit-image: image processing in Python. *Peer J*. 2014;2:e453. doi:[10.7717/peerj.453](https://doi.org/10.7717/peerj.453).
- [20] Galerne Y, Figueiredo Neto AM, Liébert L. Microscopic structure of the uniaxial and biaxial lyotropic nematics. *J Chem Phys*. 1987;87:1851–1855. doi:[10.1063/1.453199](https://doi.org/10.1063/1.453199).
- [21] Norman TJ, Grant CD, Magana D, et al. Near infrared optical absorption of gold nanoparticle aggregates. *J Phys Chem B*. 2002;106:7005–7012. doi:[10.1021/jp0204197](https://doi.org/10.1021/jp0204197).
- [22] Yang W, Liu K, Song D, et al. Aggregation-induced enhancement effect of gold nanoparticles on triplet excited state. *J Phys Chem C*. 2013;117:27088–27095. doi:[10.1021/jp410369w](https://doi.org/10.1021/jp410369w).
- [23] Delfino I. Light scattering methods for tracking gold nanoparticles aggregation induced by biotinneutravidin interaction. *Biophys Chem*. 2013;177:7–13. doi:[10.1016/j.bpc.2013.03.001](https://doi.org/10.1016/j.bpc.2013.03.001).
- [24] Esteban R, Taylor RW, Baumberg JJ, et al. How chain plasmons govern the optical response in strongly interacting self-assembled metallic clusters of nanoparticles. *Langmuir*. 2012;28:8881–8890. doi:[10.1021/la300198r](https://doi.org/10.1021/la300198r).
- [25] de Gennes PG, Prost J. *The physics of liquid crystals*, 2nd ed. The international series of monographs on physics. Oxford: Oxford University Press; 2010.
- [26] Mukherjee PK. The TNI-T\* puzzle of the nematic-isotropic phase transition. *J Phys Condens Matter*. 1998;10:9191–9205. doi:[10.1088/0953-8984/10/41/003](https://doi.org/10.1088/0953-8984/10/41/003).
- [27] Lenart VM, Gómez SL, Bechtold IH, et al. Tricritical-like behavior of the nonlinear optical refraction at the nematic-isotropic transition in the E7 thermotropic liquid crystal. *Eur Phys J E*. 2012;35:4. doi:[10.1140/epje/i2012-12004-3](https://doi.org/10.1140/epje/i2012-12004-3).
- [28] Simões M, de Campos A, Santoro PA, et al. Critical exponents at a reentrant isotropic-calamitic neinatic phase transition. *Phys Lett A*. 2004;333:120–123. doi:[10.1016/j.physleta.2004.08.066](https://doi.org/10.1016/j.physleta.2004.08.066).
- [29] de Oliveira MJ, Neto AMF. Reentrant isotropic-nematic transition in lyotropic liquid-crystals. *Phys Rev A*. 1986;34:3481–3482. doi:[10.1103/PhysRevA.34.3481](https://doi.org/10.1103/PhysRevA.34.3481).
- [30] Braga WS, Kimura NM, Luders DD, et al. Reentrant isotropiccalamitic nematic phase transition in potassium laurate-decanol-D2O mixtures. *Eur Phys J E*. 2007;24:247–250. doi:[10.1140/epje/i2007-10234-0](https://doi.org/10.1140/epje/i2007-10234-0).